

**Formation of clean dimers during gas-source growth of Si(001)**

D. R. Bowler\*

*Department of Physics and Astronomy, University College London, Gower Street, London WC1E 6BT, United Kingdom*

(Received 18 October 2002; published 31 March 2003)

Elevated temperature scanning tunneling microscopy measurements have shown that one key phase during gas-source homoepitaxy of Si(001) is the formation of clean Si ad-dimers from hydrogenated ad-dimers, though the mechanism for this formation is unknown. We present *ab initio* density functional calculations designed to explore this mechanism. The calculations show that there is a pathway consistent with the experimentally observed reaction rates, which proceeds via a metastable intermediate state, and is effectively irreversible. This result fills a vital gap in our understanding of the atomic-scale details of gas-source growth of Si(001).

DOI: 10.1103/PhysRevB.67.115341

PACS number(s): 68.43.Bc, 81.10.Aj, 81.15.Aa, 31.15.Ew

**I. INTRODUCTION**

Gas-source growth of Si(001) using hydrogen-based precursors (such as SiH<sub>4</sub>, silane, and Si<sub>2</sub>H<sub>6</sub>, disilane) is of great scientific and technological interest<sup>1-4</sup>—in particular, hydrogen can act as an effective surfactant, and has been shown to reduce roughness and intermixing during growth of Ge/Si alloys and pure Ge on Si(001).<sup>5</sup> Understanding the reactions that occur and the intermediate structures that are formed during this growth will enable greater control of surfaces and interfaces during growth. Scanning tunneling microscopy (STM) observations of the growth of Si(001) from disilane, both at room temperature following anneals<sup>1,2</sup> and at elevated temperature,<sup>3,4</sup> along with careful electronic structure calculations<sup>3,4,6</sup> have mapped out the growth pathway. A key observation in this pathway is that the islands formed during growth are *clean*, while the substrate remains covered with a certain amount of hydrogen.<sup>3</sup> The fundamental building block in gas-source growth is the clean ad-dimer (as opposed to solid-source growth, where fast-moving ad-atoms are key<sup>7</sup>); yet, the mechanism to form such clean dimers from the hydrogenated dimers that occur naturally during gas-source growth is unknown. In particular, they are observed to form at 450 K while desorption from the monohydride phase occurs at 790 K, indicating that their formation must be completely different from the desorption of hydrogen from the monohydride phase. In this paper, we present a first-principles investigation of the mechanism for formation of clean ad-dimers from hydrogenated dimers, with the aim of explaining how these form at a comparatively low temperature.

Disilane (which is used in preference to silane as it decomposes more easily) adsorbs on Si(001) as SiH<sub>3</sub> (which soon breaks down to form SiH<sub>2</sub>) or SiH<sub>2</sub>,<sup>1</sup> sometimes with accompanying hydrogen. These SiH<sub>2</sub> groups<sup>6</sup> start to diffuse at 400–500 K.<sup>3</sup> When two groups are on adjacent dimer rows, they react to form a hydrogenated ad-dimer [that is, an ad-dimer with both dangling bonds saturated with hydrogen, illustrated in Fig. 1(a)] over the trench between the dimer rows.<sup>3</sup> This then decomposes to form clean ad-dimers and hydrogen on the surface at around 450 K,<sup>1-3</sup> via a pathway to be investigated in this paper. A hydrogenated ad-dimer (which is the starting point) is illustrated in Fig. 1(a), along with a partially hydrogenated ad-dimer (the result of the first

part of the pathway) in Fig. 1(b) and a clean ad-dimer (the final point) in Fig. 1(c). Once formed, the clean ad-dimers diffuse<sup>8</sup> and form a square feature, which is believed to be the precursor to dimer strings,<sup>9</sup> followed by short strings of dimers<sup>2</sup> that later increase to form larger islands.<sup>2,4</sup> Apart from the work described above, there have not been other calculations on the growth of Si(001) from gas sources. There is work on growth from solid sources on hydrogen-terminated Si(001),<sup>10-14</sup> but interestingly this involves very different mechanisms, which are rather closer related to solid source growth on clean surfaces.

The calculations to be presented are based on density functional theory (DFT) in the generalized-gradient approximation (GGA), with a plane-wave basis set and pseudopotentials. We have searched for possible pathways both by applying constraints to specific atoms (for instance, constraining a hydrogen to lie in a given plane) and by using the nudged elastic band<sup>15,16</sup> technique (NEB), which allows accurate determination of reaction barriers given an initial approximation to a pathway. One key result is that the dehydrogenation proceeds via a metastable intermediate state (this is discussed fully in Sec. III and illustrated in Fig. 2).

The rest of the paper is organized as follows: the next section gives details of the computational techniques used; this is followed by a detailed discussion of the structure of the metastable state, which plays a key role in the dehydrogenation. The diffusion pathways are then presented, looking at the mechanism for both hydrogens, followed by a conclusion section.

**II. COMPUTATIONAL DETAILS**

The theory<sup>17,18</sup> underlying DFT and its application to electronic structure calculations have been extensively reviewed,<sup>19</sup> as has the use of pseudopotential and plane-wave techniques.<sup>20</sup> The calculations in this paper were performed using the VASP code,<sup>21</sup> using the standard ultrasoft pseudopotentials<sup>22</sup> that form part of the code. The approximation we use for exchange-correlation energy is the GGA of Perdew and Wang (PW91).<sup>23,24</sup> We chose the GGA rather than the local density approximation (LDA) rather deliberately. As the barriers that we will be calculating are sensitive to bonding and stretched bonds, and the GGA is known to be

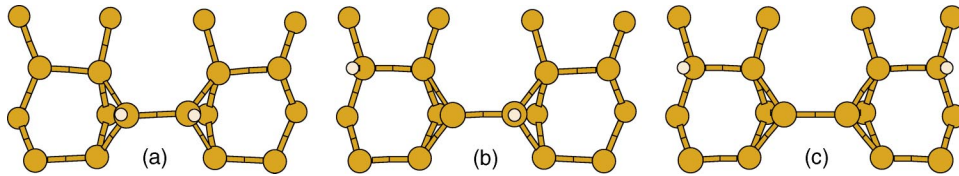


FIG. 1. Structures of (a) the starting point, with a hydrogenated ad-dimer; (b) the end point for the first diffusion event with one hydrogen on the substrate; and (c) the final point with a clean ad-dimer and both hydrogens on the substrate. Note that the asymmetry in (a) is due to the buckling of the underlying surface (up then down on the left-hand side, compared to down then up on the right-hand side).

rather more accurate in these situations (LDA generally overbinds), we considered its use to be essential for this work.

We use periodic boundary conditions, as is standard for DFT calculations with plane waves, and we therefore used a periodic slab for the surface, with a vacuum layer between the slabs. Our simulations were performed within a unit cell two dimers long and two dimer rows wide, with five layers of Si (the bottom of which was terminated in hydrogen and constrained to remain fixed in bulklike positions). The vacuum gap of 6.9 Å is equivalent to five atomic layers of Si and provides sufficient isolation between vertical periodic images. We used a plane-wave cutoff of 150 eV and a  $2 \times 2 \times 1$  Monkhorst-Pack  $k$ -point mesh. All these parameters were tested and found to converge energy differences to better than 0.01 eV. The system contains an even number of electrons, but has various saddle points that might involve unpaired electrons, so we checked the effect of performing spin-polarized calculations for these points. The effect was found to be negligible (both for energies and geometries) and so was not used in the calculations.

To investigate the diffusion pathways, we used two techniques. First, we constrained the diffusing hydrogen to lie in a particular plane and calculated static energies for different locations of the hydrogen. Second, we used the nudged elastic band method.<sup>15,16</sup> This second method requires the simultaneous relaxation of a number of images of the system, which can be done in parallel. However, this has the potential to become extremely computationally intensive, which is why we chose to use the smallest realistic unit cell (with four dimers in the surface).

The initial exploration of the system used the first method

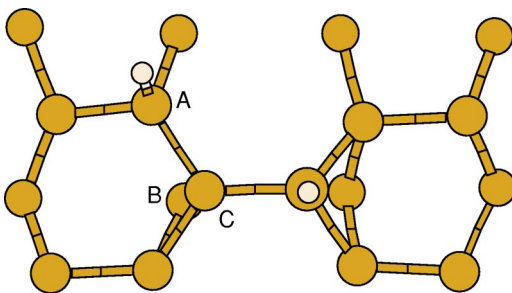


FIG. 2. The structure of the metastable state that provides a low-energy pathway for dehydrogenation. The diffusing hydrogen is bonded to a substrate dimer ( $A$ ), which has broken one bond to a second-layer silicon ( $B$ ). The ad-dimer ( $C$ ) is now partly clean and has formed a bond to the second-layer silicon ( $B$ ) left by the substrate dimer.

(static calculations, constraining the hydrogen). It was using this method that the metastable state (discussed in Sec. III) was found, and it is unlikely that it would have been found using the NEB technique without significant effort (for instance, performing simulated annealing on the initial images of the system) or using a more complicated technique such as the dimer method.<sup>25</sup> The problem of exploration of phase space is an extremely difficult one, which is discussed in more detail in Sec. V. The initial exploration was performed with the constrained method because of its simplicity—it is easy to implement and only introduces a single constraint to the system. The diffusion barriers presented in the paper were all calculated using a variant of the original technique that actively seeks the saddle point, the climbing image NEB method,<sup>26</sup> with eight images relaxed in the chain.

While we have calculated the diffusion barriers, we have not calculated attempt frequencies, which have been assumed to be  $10^{13} \text{ sec}^{-1}$ , typical for diffusion processes on semiconductor surfaces.<sup>27–29</sup> The DFT-GGA method is sufficiently accurate to calculate reaction barriers to within 0.1 eV and can be used to calculate attempt frequencies; however, the increased accuracy gained by calculating the attempt frequencies (rather than assuming them, as above) is outweighed by the cumulative errors in the calculation of both these quantities.<sup>27–30</sup> For instance, in previous work on solid-source growth of Si(001), it was shown that a factor of 5 between the attempt frequencies of competing processes was required to understand the results, but was not accurately predicted by DFT-GGA method.<sup>31</sup> We further note that, technically, free energies should be calculated, but that provided the entropy change with temperature is sufficiently small this can be rewritten in terms of an internal energy, with entropic terms absorbed in the prefactor.<sup>32</sup>

### III. THE METASTABLE INTERMEDIATE STATE

The lowest-energy diffusion pathway, and the only one that has an energy barrier that is in line with the temperature at which the dehydrogenation is observed to occur, proceeds via a metastable intermediate state. This is an unusual and rather important structure and will be discussed in detail in this section. It is illustrated in Fig. 2, and should be contrasted with the hydrogenated ad-dimer illustrated in Fig. 1(a).

The atom labeled  $A$  in Fig. 2 is one of the substrate dimers to which the hydrogenated (and clean) ad-dimer is bonded;  $B$  is a second-layer atom in the substrate to which the substrate dimer is normally bonded [for instance, in Fig. 1(a)]; and  $C$  is the ad-dimer atom itself, which is now clean (having

started hydrogenation). The hydrogen is now bonded to *A*, which has broken its bond to *B*, while *C* has formed a bond to *B* (not easily seen, owing to the geometry).

In terms of the bonding of the atoms, the atoms *A*, *B*, and *C* are all saturated as they are in Fig. 1(a)—the bonding has merely cycled around (so that the *A*—*B* bond is now an *A*—*H* bond and a *B*—*C* bond, while the *C*—*H* bond is now a *C*—*B* bond). It is this saturation that gives the structure its stability. While some of the bond angles are rather strained (in particular, the bonds associated with *B* and *C* make  $60^\circ$  angles) the bond lengths are all close to equilibrium, and there are no further broken bonds, leading to an energy difference of 0.57 eV relative to the starting point, but no more. It is interesting to note that there are other structures where  $60^\circ$  bond angles are found during growth of Si(001), which also exhibit stability that might seem counterintuitive.<sup>6</sup>

In terms of the formation of this structure, as we shall see in the next section that there is not a large barrier. The H never has to move a long distance from either *A* or *C*, leading to relatively strong bonds being present at all times; the second-layer atom *B* moves up slightly; and while the substrate dimer atom *A* and the ad-dimer atom *C* do move up and down, respectively, they do this gradually while maintaining their bonding. It is this relatively small perturbation on the overall structure, and the ease with which it is reached, that allows the formation of this state and gives it its importance.

#### IV. DIFFUSION PATHWAYS

In this section, we describe the diffusion pathways that we have explored with DFT calculations. For simplicity, and because it is likely to be physically realistic, we allow the hydrogens on the ends of the dimer to diffuse off independently, i.e., we consider the diffusion off one end of the ad-dimer while the other hydrogen remains on the ad-dimer. Then we allow the remaining hydrogen to diffuse off the now partially hydrogenated ad-dimer onto the substrate. In order to avoid the complications of spin and half-filled bands, we maintain both hydrogens in the unit cell at all times [the first hydrogen to diffuse off stays on the substrate, illustrated in Fig. 1(b)]. The three stable points of the process (fully hydrogenated ad-dimer, partially hydrogenated ad-dimer with a hydrogen on the substrate, and clean ad-dimer with both hydrogens on the substrate) are illustrated in Fig. 1. The atomic positions during the diffusion pathways are presented below in an aggregated form (due to space constraints): only the position of atoms that move significantly are shown. All of the atomic structures at each step in all the diffusion pathways are available elsewhere.<sup>33</sup>

The energies of the three stable points decrease as the hydrogen moves off the ad-dimer, which seems surprising at first. However, this can be understood in terms of two effects: first, termination of the clean ends of the substrate dimers; and second,  $\pi$  bonding of the ad-dimer. Thus in Fig. 1(c) two of the substrate dangling bonds are saturated and the ad-dimer is clean, with the two effects adding. The large stability of Fig. 1(b) over Fig. 1(a) is a little harder to understand, but arises both from the termination of one substrate

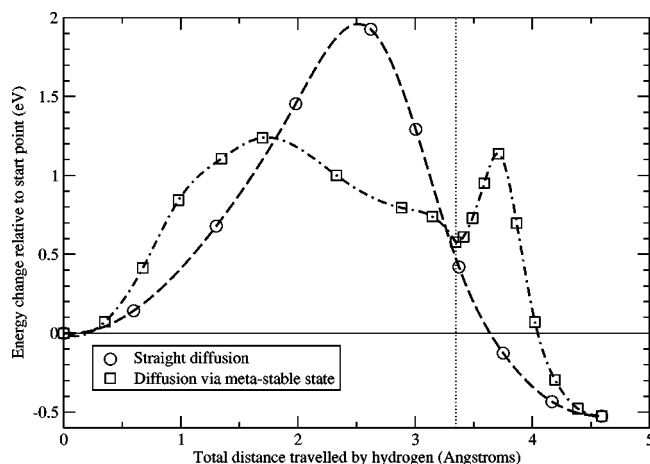


FIG. 3. A graph showing energy barriers for the diffusion for the first hydrogen off the ad-dimer. The energies are given relative to the starting point, while the *x* axis gives the distance from the starting point of the hydrogen. The open circles show direct diffusion (proceeding without the metastable intermediate state). The open squares show the diffusion via the metastable state (whose position is marked with a vertical dotted line at 3.35 Å, and whose structure is shown in Fig. 2). The lines (long dashes for direct diffusion and dash-dotted for diffusion via the metastable state) are spline fits to the data, and are given as guides to the eye.

dimer with hydrogen and from the greater variational freedom that the clean end of the ad-dimer possesses over the substrate dimers for relaxation.

The experimental data that we are comparing against comes from two separate experiments: first, where the Si(001) surface was exposed to a dose of disilane, annealed at different temperatures for different times, and then observed at room temperature in STM;<sup>1,2</sup> second, where an elevated-temperature STM experiment was used to observe the results of dosing with disilane in real time at different temperatures.<sup>3,4</sup> The results of both these types of experiment are identical: around 450 K, clean, nonrotated dimers are formed over the trench between dimer rows. In other words, the monohydride dimers lose their hydrogen to the substrate in a matter of minutes at this temperature (for instance, an anneal to 470 K for 2 min led to the dehydrogenation of all ad-dimers<sup>2</sup>). Assuming an attempt frequency of  $10^{13} \text{ sec}^{-1}$  and a successful dehydrogenation rate of  $\frac{1}{60} \text{ Hz}$ , we obtain a barrier of 1.28 eV. This changes by about 0.03 eV if the rate is doubled or halved, giving us a good estimate of the likely reaction barrier.

##### A. The first hydrogen

There are two diffusion paths considered for the first hydrogen diffusing off the ad-dimer: a direct diffusion path, and diffusion via the metastable state is considered in Sec. III and shown in Fig. 2. We will discuss these separately, starting with the direct diffusion, and then contrast their results.

The diffusion barrier for direct diffusion is shown in Fig. 3, with open circles and long dashes. The barrier is 1.93 eV, which is extremely high; the reason for this can be seen from the atomic positions, which are illustrated in Fig. 4. At the saddle point, the ad-dimer bond is extended greatly (from

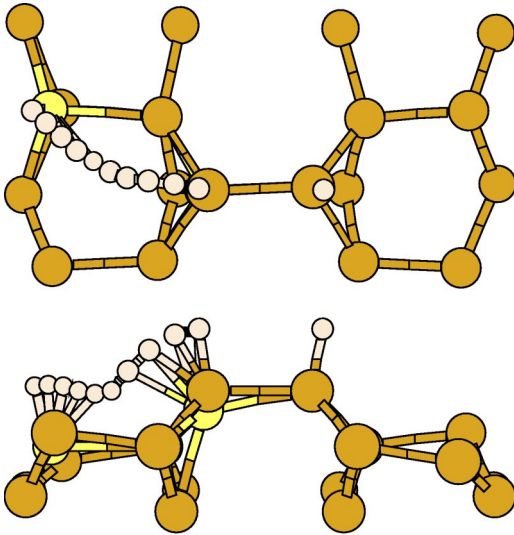


FIG. 4. The path of the first hydrogen in the direct diffusion path from above (top) and the side (bottom). All the hydrogen positions are shown, along with the initial and final positions of the atoms to which the hydrogen bonds (with the final position shown in a lighter shade). The final position of the ad-dimer cannot be seen in the top image since it is directly below the initial position. Bonds (or lack of bonds) are produced by the imaging software and should not be taken as definite indications.

2.51 Å at the start to 2.82 Å), while the bond from the hydrogen to the ad-dimer is more extended (from 1.51 Å at the start to 1.85 Å). Inspecting the charge density, it is clear that the ad-dimer remains bonded (though weakly) and that the H has made a weak bond to the substrate dimer (which is 2.32 Å away) as well as maintaining a slightly weakened bond to the ad-dimer. It is this lengthening and weakening of bonds at the saddle point that cause the high barrier. Assuming Arrhenius behavior and an attempt frequency of  $10^{13}$  Hz, we find a hopping rate of  $\sim 10^{-10}$  sec $^{-1}$  at 450 K, which is many orders of magnitude below the observed rate.

The diffusion barrier into and out of the metastable state is also shown in Fig. 3 with open squares and a dot-dashed line. The barrier from the start to the metastable state is 1.24 eV, while the barrier from the metastable state to the end is 0.56 eV (and the reverse path, from the metastable state to the start is 0.66 eV).

The pathway from the starting position to the metastable state (shown in Fig. 5) involves considerable rearrangement: First, the hydrogen inserts into the bond between the ad-dimer (labeled *C* in Fig. 2) and the substrate dimer (labeled *A* in Fig. 2); at the saddle point, the hydrogen is 1.65 Å from the ad-dimer and 1.94 Å from the substrate dimer (compared to an equilibrium distance of 1.51 Å), while the distance between the ad-dimer and the substrate dimer is 3.10 Å (compared to 2.48 Å at the start). Second, after the hydrogen has transferred to the substrate dimer, the ad-dimer bonds to a *second layer* atom in the substrate (labeled *B* in Fig. 2). Third, the substrate dimer bonds back to the ad-dimer and breaks its bond to the second layer atom in the substrate. The first part of this rearrangement is the area where most of the

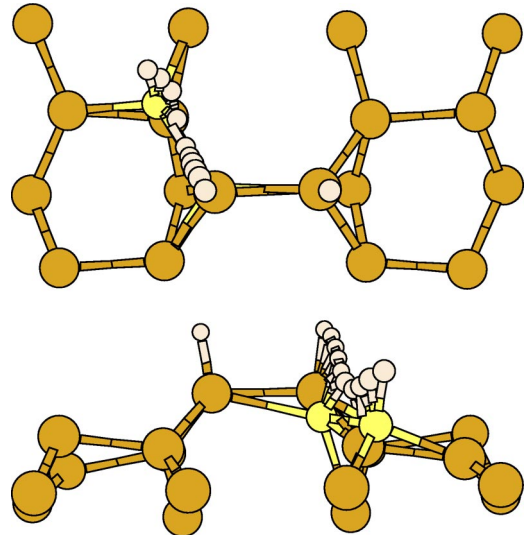


FIG. 5. The path of the first hydrogen from the ad-dimer to the metastable state shown in views from above (top) and the side (bottom). All the hydrogen positions are shown, along with the initial and final positions of the atoms to which the hydrogen bonds (with the final position shown in a lighter shade). The side view is shown rotated by 180° relative to the view from above as the image is clearer. The final position of the ad-dimer cannot be seen in the top image since it is directly below the initial position. Bonds (or lack of bonds) are produced by the imaging software, and should not be taken as definite indications.

energy change happens: the energy actually falls by about 0.6 eV during the second and third parts of the rearrangement.

The pathway from the metastable state to the end position (shown in Fig. 6) is much simpler, involving only the movement of the hydrogen from one end of the substrate dimer to the other, while the substrate dimer *C* reforms its bond to the second layer atom *B*. At the saddle point, the hydrogen is 1.72 Å from the substrate atom and 2.05 Å from the end atom.

The barrier of 1.24 eV from the starting point to the metastable state fits extremely well with the observed temperature behavior: at 450 K with an attempt frequency of  $10^{13}$  sec $^{-1}$ , it would correspond to a hopping rate of 0.044 Hz, or one hop every 23 sec. But this is only *into* the metastable state, and there are *two* low-energy paths out of that. The hopping rate from the metastable state to the end state is  $\sim 4 \times 10^6$  Hz, while from the metastable state to the start state is  $\sim 2 \times 10^5$  Hz, so that only 10% of metastable states would return to the starting point. We also expect that the equilibrium populations of the start and end states would differ, since the end state is 0.53 eV lower than the start (roughly, at 450 K, we would expect a relative population about  $10^6$  times higher in the lower state). There is also the question of whether the hydrogen could return, via the metastable state, from the end to the start. The barrier from the end point *back* to the metastable state is 1.66 eV, making it extremely unlikely that the hydrogen would return to the metastable state (and even if it did, it would be 10 times more likely to drop back to the end state than to return to the start state). Clearly,

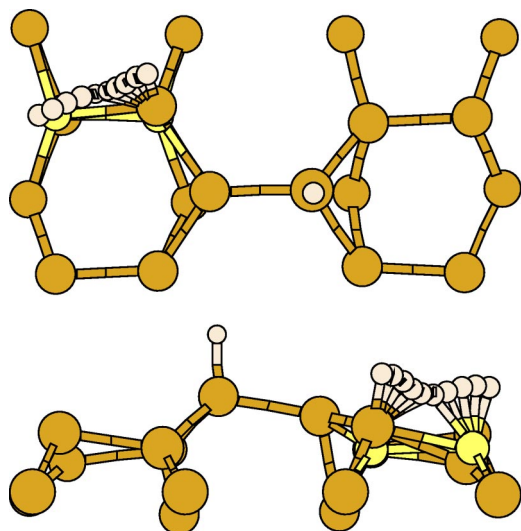


FIG. 6. The path of the first hydrogen from the metastable state to the substrate dimer shown in views from above (top) and the side (bottom). All the hydrogen positions are shown, along with the initial and final positions of the atoms to which the hydrogen bonds (with the final position shown in a lighter shade). The side view is shown rotated by  $180^\circ$  relative to the view from above as the image is clearer. Bonds (or lack of bonds) are produced by the imaging software, and should not be taken as definite indications.

it is the low barrier from the starting state to the metastable state that allows the first part of the dehydrogenation of the ad-dimer to proceed, and the energy difference between the start and end points, as well as the high barrier out of the end state, that makes the reaction effectively irreversible.

### B. The second hydrogen

Once the first hydrogen has diffused off the ad-dimer, we retain it on the substrate, as shown in Fig. 1(b). This is computationally convenient (as it maintains a filled set of bands) but also physically reasonable: hydrogen does not begin diffusing along the dimer rows on Si(001) at an appreciable rate until about 550 K with a barrier of 1.68 eV.<sup>34</sup>

As with the first hydrogen, the second hydrogen can diffuse either directly or via a metastable state, which is exactly equivalent to the metastable state for the first hydrogen (shown in Fig. 2) and therefore not illustrated here. As before, we will discuss these results separately, starting with the direct diffusion.

The diffusion barrier for direct diffusion is shown in Fig. 7, plotted with open circles and dashes. The shape is much broader than that for the first hydrogen's direct path, with a lower barrier of 1.59 eV. The reason for this can be seen in part in the atomic positions, which are shown in Fig. 8. This is slightly more confusing than previous plots, as the positions both of the hydrogen and the ad-dimer atom to which it is bonded have been plotted. As the hydrogen moves across towards the substrate dimer (the end point), the bond between the silicon atoms in the ad-dimer breaks, with the atom that the hydrogen is bonded to following the hydrogen as it diffuses. At the saddle point, the hydrogen is 1.67 Å from the ad-dimer and 2.03 Å from the substrate dimer,

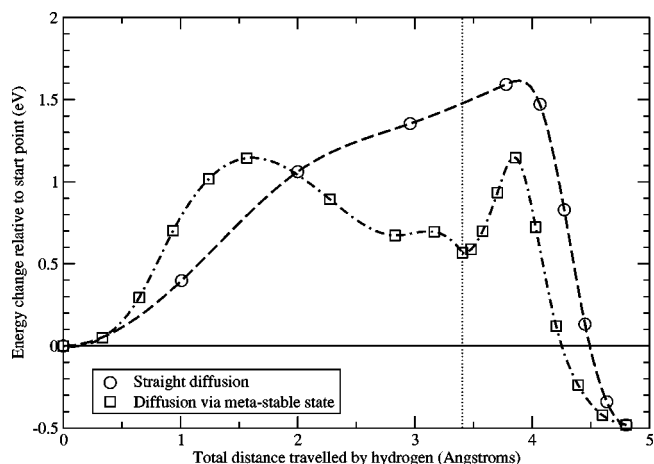


FIG. 7. A graph showing energy barriers for the diffusion of the second hydrogen off the ad-dimer (with the first hydrogen already on the substrate). The energies are given relative to the starting point, while the  $x$  axis gives the distance from the starting point of the hydrogen. The open circles show direct diffusion (proceeding without the metastable intermediate state). The open squares show the diffusion via the metastable state (whose position is marked with a vertical dotted line at 3.41 Å, and whose structure is shown in Fig. 2). The lines (long dashes for direct diffusion and dash-dotted form for diffusion via the metastable state) are spline fits to the data and are given as guides to the eye.

while the distance between ad-dimer atoms is 4.48 Å. Beyond this point, the hydrogen transfers to the substrate, and the ad-dimer reforms slowly.

The bond in the clean or partially clean ad-dimer is not as strong as the other bonds to the substrate, which explains why the energy cost for breaking it is relatively small, and why this pathway is followed in contrast to the pathway for

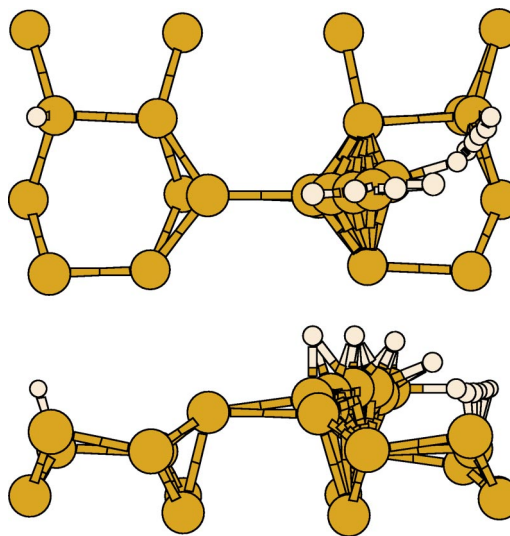


FIG. 8. The path of the second hydrogen in the direct diffusion path shown in views from above (top) and the side (bottom). All the hydrogen positions are shown, as are the positions of the atoms to which the hydrogen bonds. Bonds (or lack of bonds) are produced by the imaging software and should not be taken as definite indications.

the first hydrogen. Even with the reduced barrier, the hopping rate at 450 K will be  $\sim 4 \times 10^{-6} \text{ sec}^{-1}$ , which is still far too low to be consistent with the experimental observations.

The diffusion barrier into and out of the metastable state is also shown in Fig. 7, plotted with open squares and dot-dashed lines. The barrier from the start to the metastable state is 1.14 eV, while the barrier from the metastable state to the end is 0.58 eV (and the reverse path, from the metastable state to the start is also 0.58 eV). The atomic positions are almost identical to those for the first diffusion (shown in Figs. 5 and 6) and are not shown (though these figures, and many other pieces of supplementary information such as animations of the processes can be found elsewhere<sup>33</sup>).

The barrier of 1.14 eV is 0.1 eV lower than the barrier for the first hydrogen, suggesting that once the first hydrogen has diffused off the ad-dimer, the second will follow slightly more quickly; it is still in excellent agreement with observed experimental behavior. The barriers from the metastable state to the start and end states are now identical, meaning that 50% of metastable states will return to the starting state. However, the end state is 0.48 eV lower in energy than the start, so that (as before with the first hydrogen) we would expect the population in thermal equilibrium at 450 K to be about  $10^6$  times higher in the end state than the start state. The barrier from the end state back to the metastable state is 1.63 eV, which again makes the reaction effectively irreversible. Of course, the clean ad-dimer can also diffuse away along the trench between dimer rows, with a barrier of 1.15 eV,<sup>8</sup> which would make the reforming of the hydrogenated ad-dimer impossible.

## V. CONCLUSIONS

We have presented *ab initio* calculations, modeling the diffusion of hydrogen off a hydrogenated ad-dimer, which is a key stage in gas-source growth of Si(001). We have shown that the diffusion proceeds via a metastable intermediate state, and that the energy barriers calculated (1.24 eV for the

first hydrogen and 1.14 eV for the second hydrogen) are in excellent agreement with temperatures at which these features are observed in experiment. A detailed knowledge of the mechanisms of growth will enable closer control of the growth process, as well as other applications. The development of *ab initio* kinetic Monte Carlo applications,<sup>28,29</sup> where the barriers are derived from DFT or other calculations, is becoming common, and there is now nearly enough information to develop such a model for gas-source growth of Si(001). It also allows the development of new experimental growth approaches such as atomic layer epitaxy through saturation with monohydride dimers.<sup>35</sup>

We have used the climbing image nudged elastic band method to find the diffusion barriers, and have found it to be extremely effective, particularly for the direct diffusion, which was difficult to model simply by picking a single constraint. However, the problem of exploring phase space is still a difficult one, as the existence of the metastable state (which was discovered through application of a single constraint) shows. Indeed, although two pathways for dehydrogenation have been presented, there is no way of knowing if these are the only mechanisms, though the close correspondence between the experimental and theoretical barriers suggests that the pathway via the metastable state would make a large contribution to the dehydrogenation process. There are techniques for exploring energy surfaces, such as the dimer method<sup>25</sup> and variants on hyperdynamics,<sup>36</sup> but there is still a large amount of work to be done in this field.

## ACKNOWLEDGMENTS

We gratefully acknowledge useful discussions with Dr J.H.G. Owen, Dr. C.M. Goringe and Professor M.J. Gillan. D.R.B. is funded by the Royal Society. Calculations were performed at the HiPerSPACE Centre, UCL, which is partly funded by JREI Grant No. JR98UCGI. We also acknowledge the Jónsson group in University of Washington for making their implementation of the NEB and climbing image NEB within VASP publicly available.

\*Also at London Center for Nanotechnology, Gordon St, London WC1E 6BT. Electronic address: david.bowler@ucl.ac.uk  
<sup>1</sup>M.J. Bronikowski, Y. Wang, M.T. McEllistrem, D. Chen, and R.J. Hamers, *Surf. Sci.* **298**, 50 (1993).  
<sup>2</sup>Y. Wang, M.J. Bronikowski, and R.J. Hamers, *Surf. Sci.* **311**, 64 (1994).  
<sup>3</sup>J.H.G. Owen, K. Miki, D.R. Bowler, C.M. Goringe, I. Goldfarb, and G.A.D. Briggs, *Surf. Sci.* **394**, 79 (1997).  
<sup>4</sup>J.H.G. Owen, K. Miki, D.R. Bowler, C.M. Goringe, I. Goldfarb, and G.A.D. Briggs, *Surf. Sci.* **394**, 91 (1997).  
<sup>5</sup>N. Ohtani, S. Mokler, M.H. Xie, J. Zhang, and B.A. Joyce, *Jpn. J. Appl. Phys., Part 1* **33**, 2311 (1994).  
<sup>6</sup>D.R. Bowler and C.M. Goringe, *Surf. Sci. Lett.* **360**, L489 (1996).  
<sup>7</sup>B.S. Swartzentruber, *Phys. Rev. Lett.* **76**, 459 (1996).  
<sup>8</sup>C.M. Goringe and D.R. Bowler, *Phys. Rev. B* **56**, R7073 (1997).  
<sup>9</sup>J.H.G. Owen, D.R. Bowler, C.M. Goringe, K. Miki, and G.A.D. Briggs, *Surf. Sci. Lett.* **382**, L678 (1997).  
<sup>10</sup>J. Nara, T. Sasaki, and T. Ohno, *Phys. Rev. Lett.* **79**, 4421 (1997).

<sup>11</sup>J. Nara, T. Sasaki, and T. Ohno, *Appl. Surf. Sci.* **130-132**, 254 (1998).  
<sup>12</sup>J. Nara, T. Sasaki, and T. Ohno, *J. Cryst. Growth* **201-202**, 77 (1999).  
<sup>13</sup>J. Nara, T. Ohno, H. Kajiyama, and T. Hashizume, *Appl. Surf. Sci.* **162-163**, 152 (2000).  
<sup>14</sup>S. Jeong and A. Oshiyama, *Appl. Surf. Sci.* **130-132**, 287 (1998).  
<sup>15</sup>H. Jónsson, G. Mills, and K.W. Jacobsen, in *Classical and Quantum Dynamics in Condensed Phase Simulations*, edited by B.J. Berne, G. Cicciotti, and D.F. Coker (World Scientific, Singapore, 1998), p. 385.  
<sup>16</sup>G. Henkelman, B. Uberaga, and H. Jónsson, *J. Chem. Phys.* **113**, 9978 (2000).  
<sup>17</sup>P. Hohenberg and W. Kohn, *Phys. Rev.* **136**, B864 (1964).  
<sup>18</sup>W. Kohn and L.J. Sham, *Phys. Rev.* **140**, A1133 (1965).  
<sup>19</sup>R.O. Jones and O. Gunnarsson, *Rev. Mod. Phys.* **61**, 689 (1989).  
<sup>20</sup>M.C. Payne, M.P. Teter, D.C. Allan, T.A. Arias, and J.D. Joannopoulos, *Rev. Mod. Phys.* **64**, 1045 (1992).

- <sup>21</sup>G. Kresse and J. Furthmüller, Phys. Rev. B **54**, 11 169 (1996).
- <sup>22</sup>D. Vanderbilt, Phys. Rev. B **41**, 7892 (1990).
- <sup>23</sup>Y. Wang and J.P. Perdew, Phys. Rev. B **44**, 13 298 (1991).
- <sup>24</sup>J.P. Perdew, J.A. Chevary, S.H. Vosko, K.A. Jackson, M.R. Pederson, D.J. Singh, and C. Fiolhais, Phys. Rev. B **46**, 6671 (1992).
- <sup>25</sup>G. Henkelman and H. Jónsson, J. Chem. Phys. **111**, 7010 (1999).
- <sup>26</sup>G. Henkelman, B. Uberaga, and H. Jónsson, J. Chem. Phys. **113**, 9901 (2000).
- <sup>27</sup>A. Kley, P. Ruggerone, and M. Scheffler, Phys. Rev. Lett. **79**, 5278 (1997).
- <sup>28</sup>P. Kratzer and M. Scheffler, Phys. Rev. Lett. **88**, 036102 (2002).
- <sup>29</sup>F. Grosse and M.F. Gyure, Phys. Rev. B **66**, 075320 (2002).
- <sup>30</sup>P.E. Blöchl, C. van de Walle, and S.T. Pantelides, Phys. Rev. Lett. **75**, 469 (1990).
- <sup>31</sup>A.P. Smith and H. Jónsson, Phys. Rev. Lett. **77**, 1326 (1996).
- <sup>32</sup>G.H. Vineyard, J. Phys. Chem. Solids **3**, 121 (1957).
- <sup>33</sup>Further information, including animations, can be found at the following web page: <http://www.cmp.ucl.ac.uk/~drb/Research/DeHydro.html>.
- <sup>34</sup>J.H.G. Owen, D.R. Bowler, C.M. Goringe, K. Miki, and G.A.D. Briggs, Phys. Rev. B **54**, 14 153 (1996).
- <sup>35</sup>Y. Suda, Y. Misato, D. Shiratori, K. Oryu, and M. Yamashita, Appl. Surf. Sci. **130-132**, 304 (1998).
- <sup>36</sup>A. Voter, Phys. Rev. Lett. **78**, 3908 (1997).